



Minerva Access is the Institutional Repository of The University of Melbourne

Author/s:

Zaccarian, L;Nesic, D;Teel, AR

Title:

Explicit Lyapunov functions for stability and performance characterizations of FOREs connected to an integrator

Date:

2006

Citation:

Zaccarian, L., Nesic, D. & Teel, A. R. (2006). Explicit Lyapunov functions for stability and performance characterizations of FOREs connected to an integrator. Proceedings of the 45th IEEE Conference on Decision and Control, pp.771-776. IEEE. <https://doi.org/10.1109/CDC.2006.377821>.

Persistent Link:

<https://hdl.handle.net/11343/301353>

# Explicit Lyapunov functions for stability and performance characterizations of FOREs connected to an integrator

Luca Zaccarian, Dragan Nešić and Andrew R. Teel

**Abstract**—In this paper we provide explicit Lyapunov functions that prove that a First Order Reset Element (FORE) in negative feedback interconnection with an integrator is exponentially stable for any, positive or negative, value of the pole of the FORE. The Lyapunov functions also allow to establish finite gain  $\mathcal{L}_2$  stability from a disturbance input acting at the input of the plant to the plant output.  $\mathcal{L}_2$  stability is established by giving a bound on the corresponding  $\mathcal{L}_2$  gains. The framework used for the characterization of the system dynamics and for the stability and performance analysis corresponds to the ideas first proposed in (Nesic et al. IFAC 2005) and (Zaccarian et al. ACC 2005).

## I. INTRODUCTION

First Order Reset Elements (FOREs) correspond to first order linear systems whose state is reset to zero whenever the input and the state values have opposite signs. First order reset elements were first introduced in [11] as a generalization of the so-called Clegg integrator [6], [15] which is the special case of a FORE having its pole at the origin. Despite their early origins (the first scheme of [6] was presented still in the analog controllers era), reset controllers didn't capture much attention until recent years. Perhaps because the mathematical tools for describing the dynamics behind reset linear systems were not yet advanced enough. A nice summary of the early research results on reset control systems is given in the recent paper [3].

Reset controllers reach beyond the use of classical linear and nonlinear control schemes because the state response of the closed-loop is a discontinuous function of time (due to the occurrence of resets). If on one hand this fact becomes a difficulty for the analysis of stability and performance, on the other hand, it is a peculiarity that may allow in certain cases to achieve performance specifications that outperform the intrinsic limitations of classical control architectures (see [1], [7]). A nice feature of reset control systems is that they are well described as hybrid systems, namely systems whose dynamics are governed by the combination of a flow map

of the type  $\dot{x} = f(x, v)$ , only active in certain subsets of the state space, called the *flow set* and a jump map of the type  $x^+ = g(x, v)$  which is active in another subset of the state space, called the *jump set*. A necessary requirement of the corresponding description is that the union of the flow and the jump set coincides with the whole state space, so that existence of solutions will be guaranteed for any initial conditions. In fact, the matter of existence of solutions for hybrid systems in general and reset systems as a special case has been addressed in many different ways in the recent literature and one of the main issues is to rule out solutions that jump infinitely many times on compact time intervals (the so-called Zeno solutions).

Several approaches have been taken in the recent literature to model control systems involving FOREs, so that formal statements about their stability and performance could be proved. Some recent works (see, [12], [10], [4]) rely on explicit characterization of the reset time, but this only applies to second order systems. For higher order systems, the trajectories are seen as a patching of different pieces between reset times (this is why Zeno solutions need to be ruled out) and patching them together (see, [9], [5], [2]). In [16], [17], we proposed a novel interpretation of reset systems, both in terms of the characterization of the flow and jump sets and in terms of the notation used to characterize the hybrid systems dynamics. In particular, for the first time, we recognized in [17] that the analog circuit first proposed in [6] for the Clegg integrator was forced to reset in half of the state space, so that trajectories weren't allowed to flow in a very large set. Moreover, adopting the hybrid representation for solutions proposed in [8], allowed us to cast the problem of exponential stability as a problem of robust exponential stability (where the distance between solutions was redefined, as in [8] relying on hybrid domains). This new framework allowed us to introduce novel stability and performance conditions for FORE control systems and to establish for the first time results about exponential stability and  $\mathcal{L}_2$  performance of reset systems that would be exponentially stable without resets (see [16], [17] for details).

In [16], [17] we addressed and solved the problem of Zeno solutions by introducing the so-called “temporal regularization” within our dynamic equations. Temporal regularization, also used in [13], [4], corresponds to not allowing resets unless a certain time interval  $\rho > 0$  has passed since the last reset. It is straightforward that updating the jump and flow rules with this extra constraint referring to a new state variable  $\tau(t)$  whose flow equation is  $\dot{\tau} = 1$  rules out Zeno solutions because in any compact time interval of length  $T$

Work supported in part by ARC under the Australian Professorial Fellowship and Discovery Grant DP DP0451177, ARO under Grant no. DAAD19-03-1-0144, NSF under Grants no. CCR-0311084 and ECS-0324679, AFOSR under Grant no. FA9550-06-1-0134, ENEA-Euratom and MIUR under PRIN and FIRB projects.

D. Nešić is with the Electrical and Electronic Engineering Department, University of Melbourne, Parkville 3010 Vic., Australia [d.nesic@ee.mu.oz.au](mailto:d.nesic@ee.mu.oz.au)

A.R. Teel is with the Department of Electrical and Computer Engineering, University of California, Santa Barbara, CA 93106, USA [teel@ece.ucsb.edu](mailto:teel@ece.ucsb.edu)

L. Zaccarian is with the Dipartimento di Informatica, Sistemi e Produzione, University of Rome, Tor Vergata, 00133 Rome, Italy [zack@disp.uniroma2.it](mailto:zack@disp.uniroma2.it)

there can be no more than  $T/\rho$  resets. The same technique will be used here.

In this paper we report on new developments about reset control systems with FOREs. In particular we focus on the simplest example of a FORE connected to an integrator and we characterize stability and  $\mathcal{L}_2$  performance of the closed-loop for all values of the FORE pole by way of a pair of parametric Lyapunov functions. We also comment on how the analytic bounds herein obtained compare to the numerical bounds obtained by using the techniques of [17].

The paper is structured as follows: in Section II we give the dynamic equations of a FORE controlling an integrator. In Section III we state our main theorem and compare the corresponding bounds to the numerical bounds of [17] in addition to giving some intuition about the meaning of certain trends in the  $\mathcal{L}_2$  gains. Finally, in Section IV we prove our main result.

## II. A FORE CONTROLLING AN INTEGRATOR

In this section, we discuss on how the Clegg integrator model developed in the previous sections extend to the case of reset control system involving a first order reset element (FORE) controlling an integrator. If a disturbance affects the plant input, the plant dynamics can be represented as

$$\dot{y} = u + d, \quad (1)$$

where  $u$  is the control input,  $d$  is a disturbance input and  $y$  is the plant state and output.

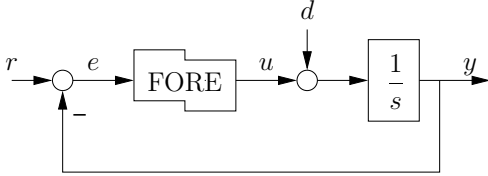


Fig. 1. An integrator controlled by a FORE.

For the plant (1), assume that a control system is designed, according to Figure 1, where the FORE element is described by the following dynamics:

$$\text{FORE} \begin{cases} \dot{x}_r = \lambda_r x_r + e, & \text{if } ex_r \geq 0 \\ x_r^+ = 0, & \text{if } ex_r \leq 0, \end{cases} \quad (2)$$

$$\text{Interconnection} \begin{cases} u = x_r, \\ e = r - y \end{cases} \quad (3)$$

where  $r$  is the reference input,  $\lambda_r \in \mathbb{R}$  denotes the time constant of the FORE. Note that  $\lambda_r$  can be any number (including positive ones). Choosing  $k = 1$  and  $\lambda_r = 0$  corresponds to implementing in the FORE the Clegg integrator commented in Section I.

The overall closed-loop system augmented with the temporal regularization can then be described by the following

equations for  $x := [y \ x_r]^T$ :

$$\begin{cases} \dot{\tau} = 1, \\ \dot{x} = Ax + B_d d + B_r r, & \text{if } x^T M x \geq 0 \text{ or } \tau \leq \rho, \\ \tau^+ = 0, \\ x^+ = A_r x, & \text{if } x^T M x \leq 0 \text{ and } \tau \geq \rho, \\ y = Cx \end{cases} \quad (4)$$

where  $A$  denotes the flow matrix,  $A_r$  denotes the reset matrix and  $M$  characterizes the flow and the jump sets (note that these two sets have their boundaries in common). Based on the values in (1), (2) and (3), the matrices in (4) are

$$\begin{aligned} A &= \begin{bmatrix} 0 & 1 \\ -1 & \lambda_r \end{bmatrix}, & B_d &= \begin{bmatrix} 1 \\ 0 \end{bmatrix}, & B_r &= \begin{bmatrix} 0 \\ 1 \end{bmatrix}, \\ A_r &= \begin{bmatrix} 1 & 0 \\ 0 & 0 \end{bmatrix}, & M &= \begin{bmatrix} 0 & -1 \\ -1 & 0 \end{bmatrix}, \\ C &= \begin{bmatrix} 1 & 0 \end{bmatrix}. \end{aligned} \quad (5)$$

## III. GAIN ESTIMATION VIA ANALYTIC CONSTRUCTION OF LYAPUNOV FUNCTIONS

One of the big advantages of the models introduced in [16], [17] and recalled in the previous section stands in the fact that the search for Lyapunov functions guaranteeing stability properties can be carried out by only imposing the flow condition in a subset of the state space and then patching the Lyapunov level sets with an extra piece which satisfies the jump condition. This idea can be exploited to analytically construct a Lyapunov function. We address here the simple, yet very relevant case of a FORE connected to an integrator. This planar system has been widely studied in the literature and its improved  $\mathcal{L}_2$  performance properties are here characterized by way of a pair of analytic Lyapunov functions. The bounds corresponding to equation (7) are graphically represented in Figure 2 in the following section, where they are compared to the bounds obtained by using the numerical optimization tools proposed in [17].

*Proposition 1:* Given any  $\lambda_r \in \mathbb{R}$ , Consider the closed-loop between

$$\dot{y} = u + d, \quad (6)$$

and the FORE (2), (3) with temporal regularization. Then for any (positive or negative) value of  $\lambda_r \in \mathbb{R}$ , the closed-loop system is exponentially stable and a bound (depending on the FORE's pole  $\lambda_r$ ) for the  $\mathcal{L}_2$  gain estimate from  $d$  to  $y$  is given by:

$$\gamma(\lambda_r) \leq \begin{cases} \frac{2}{|\lambda_r|} + |\lambda_r|, & \text{if } \lambda_r < 0, \\ \max \left\{ \frac{\pi}{2}, \frac{2\pi}{4 + \pi\lambda_r} \right\}, & \text{if } \lambda_r > -\frac{4}{\pi}. \end{cases} \quad (7)$$

*Proof:* See Section IV. ■

*Remark 1:* (Comparing analytic and numerical bounds) In Figure 2, the  $\mathcal{L}_2$  bounds obtained in Theorem 1 for different values of  $\lambda_r$  are compared to the numerical bounds obtained by applying the numerical results proposed in [17]. Note that the numerical bounds are always tighter than the analytic ones, however, the relevance of the analytic results stands in the fact that exponential stability and a bound on the  $\mathcal{L}_2$  gain is proved for all values of  $\lambda_r$ , whereas the numerical

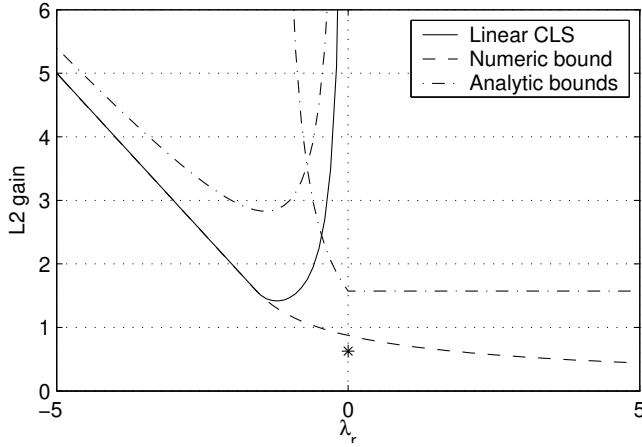


Fig. 2. The  $\mathcal{L}_2$  gain estimates obtained by using PWQ Lyapunov functions (solid) of [17] for different values of the FORE's pole  $\lambda_r$ , compared to the corresponding linear performance (dashed) and to the analytic bounds established in Theorem 1 (dash-dotted).

tools of [17] lead to infeasibility for positive values of  $\lambda_r$  that become too large.  $\circ$

*Remark 2:* (A lower bound on the  $\mathcal{L}_2$  gain for  $\lambda_r = 0$ ) An interesting question corresponds to asking how tight the analytic and numerical bounds in Figure 2 are. A partial answer to this question is given by the following result which establishes that for the case  $\lambda_r = 0$  (namely, the Clegg integrator), the gain is not smaller than  $\sqrt{\pi/8} \approx 0.626$ , which coincides with the star reported in Figure 2. Note that the numerical upper bound determined by [17] is extremely close to this lower bound.

To show this property for the gain, consider the closed-loop without temporal regularization (the extension is trivial) given by

$$\begin{aligned} \dot{y} &= x_r + d, \\ \dot{x}_r &= -y, \end{aligned} \quad (8)$$

and select the following initial conditions  $y(0) \in \left(\frac{\sqrt{2}}{2}, 0\right)$ ,  $x_r(0) = -y(0)$ . Then select the following disturbance:

$$d(t) = \begin{cases} 2 \exp(t)y(0) & t \in [0, t^*], \\ 0 & t > t^*, \end{cases}$$

where  $t^* := \ln\left(\frac{\sqrt{2}}{-2y(0)}\right)$ . Then it is immediate to check that

$$\begin{aligned} \|d\|_2 &= \sqrt{4 \cdot \frac{1}{2} [\exp(2t^*) - 1] y^2(0)} \\ &\leq \sqrt{2} |\exp(t^*) y(0)| = 1. \end{aligned}$$

and that in the limit as  $y(0) \rightarrow 0$ ,  $\|d\|_2 \rightarrow 1$ . Then, by substituting in (8) and considering that  $x_r(t) = -\exp(t)y(0)$ , the following holds:

$$y(t) = \begin{cases} \exp(t)y(0) & t \in [0, t^*], \\ -\cos(t - t^* + \pi/4) & t \in [t^*, t^* + \pi/4]. \end{cases}$$

It follows that in the first time interval  $[0, t^*]$ , since  $y(t) = 0.5d(t)$ , we have

$$\|y_{[0, t^*]}\|_2^2 = \frac{1}{2} [\exp(2t^*) - 1] y^2(0),$$

and that in the limit as  $y(0) \rightarrow 0$ ,  $\|y_{[0, t^*]}\|_2^2 \rightarrow 1/4$ . For the remaining time interval, we have

$$\begin{aligned} \|y_{[t^*, t^* + \pi/4]}\|_2^2 &= \int_{\pi/4}^{\pi/2} \cos^2(\tau) d\tau \\ &= \left| \frac{1}{2}t + \frac{1}{4} \sin(2t) \right| \\ &= \frac{\pi}{4} - \frac{\pi}{8} - \frac{1}{4}. \end{aligned}$$

Since the state is reset to zero and remains there after  $t^* + \pi/4$ , then, in the limit as  $y(0) \rightarrow 0$ , we have

$$\|y\|_2 \rightarrow \sqrt{\frac{\pi}{8}} = \sqrt{\frac{\pi}{8}} \|d\|_2,$$

which proves the claim.  $\circ$

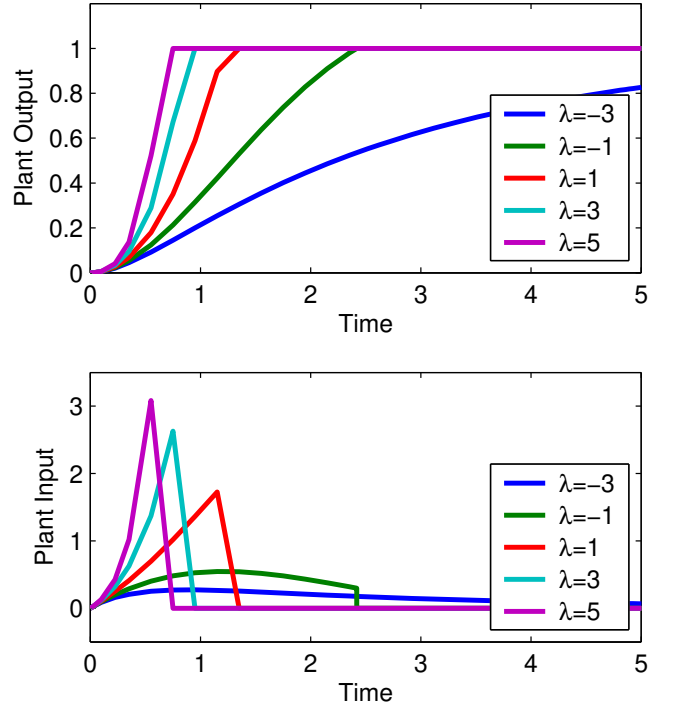


Fig. 3. Simulations of step responses of closed-loops between FOREs and an integrator for different values of  $\lambda_r$ .

*Remark 3:* (From intuition to formalization) The results of Theorem 1 correspond to the mathematical formalization of the following intuitive reasoning about the closed-loop behavior of the control system of Figure 1. Since the plant is an integrator, then the linear part of the control system will always correspond to trajectories that spiral around the origin of the phase plane. Having  $\lambda_r = 0$  will correspond to closed trajectories (circles in the phase plane),  $\lambda_r < 0$  will lead to exponentially stable trajectories spiraling inward toward the origin and  $\lambda_r > 0$  will lead to exponentially unstable trajectories spiraling outward toward infinity. When resets come to place, any of these stable and unstable trajectories will be blocked when they approach the second and fourth quadrant, and will be reset to zero, no matter what the value of  $\lambda_r$  is. Therefore, the conclusion about

exponential stability established in Theorem 1. Let's consider now the bounds on the  $\mathcal{L}_2$  gain from  $d$  to  $y$ . Large negative values of  $\lambda_r$  will correspond to exponentially stable branches of trajectories that move very slowly toward the resetting quadrants, therefore the  $\mathcal{L}_2$  gain of the corresponding closed-loops will be larger and larger as  $\lambda_r$  becomes more and more negative (see also the very left of Figure 2). The decreasing trend of the gain as  $\lambda_r$  approaches zero only occurs up to a certain point in the linear case because the linear trajectories approach the unstable cases (occurring with  $\lambda_r > 0$ ). Conversely, in the reset case, the branches approaching the reset quadrants become increasingly fast and steep, even for positive values of  $\lambda_r$ . The corresponding gain becomes then smaller and smaller. This trend is easily understood by inspecting the simulations of Figure 3, where several step responses (corresponding to increasing values of  $\lambda_r$ ) are reported. From these simulations it becomes evident that as  $\lambda_r$  approaches  $+\infty$ , the step responses approach a step output (so that the gain approaches zero) because they correspond to an increasingly fast exponentially unstable branch up to the desired set-point, followed by a constant branch. The decreasing trend of the gain as  $\lambda_r$  approaches  $+\infty$  is confirmed by the numerical results, whereas the bound provided by our Lyapunov approach is non decreasing. Recent preliminary results reveal that should be possible to prove analytically that the  $\mathcal{L}_2$  gain from  $d$  to  $y$  indeed approaches zero as  $\lambda_r$  approaches  $+\infty$ .  $\circ$

#### IV. PROOF OF PROPOSITION 1

In [16] Lyapunov-based results for a general class of reset systems have been given. These results allow us to establish exponential stability of the closed-loop and  $\mathcal{L}_2$  performance properties. The main result of [16] can be written as follows for the special reset control system in (4), when only focusing on second order homogeneous Lyapunov functions.

*Theorem 1:* [16] Consider the reset control system (4) with the matrix selection (5). Select either  $w = r$  and  $B_w = B_r$  or  $w = d$  and  $B_w = B_d$ . Assume that there exists a locally Lipschitz function  $V(x) := x^T P(x)x$ , and strictly positive constants  $a_1, a_2, \gamma, \varepsilon_M$  and  $\varepsilon_S$ , such that

- 1)  $a_1|x|^2 \leq V(x) \leq a_2|x|^2$  for all  $x \in \mathbb{R}^n$ ,
- 2)  $P(\lambda x) = P(x) = P^T(x) > 0$  for all  $x \in \mathbb{R}^n \setminus \{0\}$  and for all  $\lambda \in \mathbb{R}$ ,
- 3)  $\frac{\partial V(x)}{\partial x}(Ax + B_w w) + \varepsilon_S|x|^2 + \frac{1}{\gamma}|y|^2 - \gamma|w|^2 < 0$ , for almost all  $x$  such that  $x^T(M + \varepsilon_M I)x \geq 0$ ,
- 4)  $V(A_r x) - V(x) \leq 0$  for all  $x$  such that  $x^T M x \leq 0$ .

Then there exists a small enough  $\rho^* > 0$  such that for any fixed  $\rho \in (0, \rho^*)$ , the FORE control system (4) is exponentially stable and has a finite  $\mathcal{L}_2$  gain from  $w$  to  $y$  which is smaller than  $\gamma$ .

*Remark 4:* The condition at item 2 corresponds to requiring that the Lyapunov function is homogeneous of degree two. The condition at item 3 corresponds to requiring that in a set that is slightly larger than the flow set the Lyapunov function is a disturbance attenuation Lyapunov function for the input  $w$  and the output  $y$ . The condition at item 4

corresponds to requiring that the Lyapunov function does not increase along resets. As compared to the main result in [16], Theorem 1 does not explicitly require that immediately after the resets the closed-loop state belongs to the flow set. Indeed, since resets will always drive the FORE state to zero, the state after reset will necessarily belong to the flow set (by the structure of  $M$ ) and no extra requirement is needed on the resetting strategy.  $\circ$

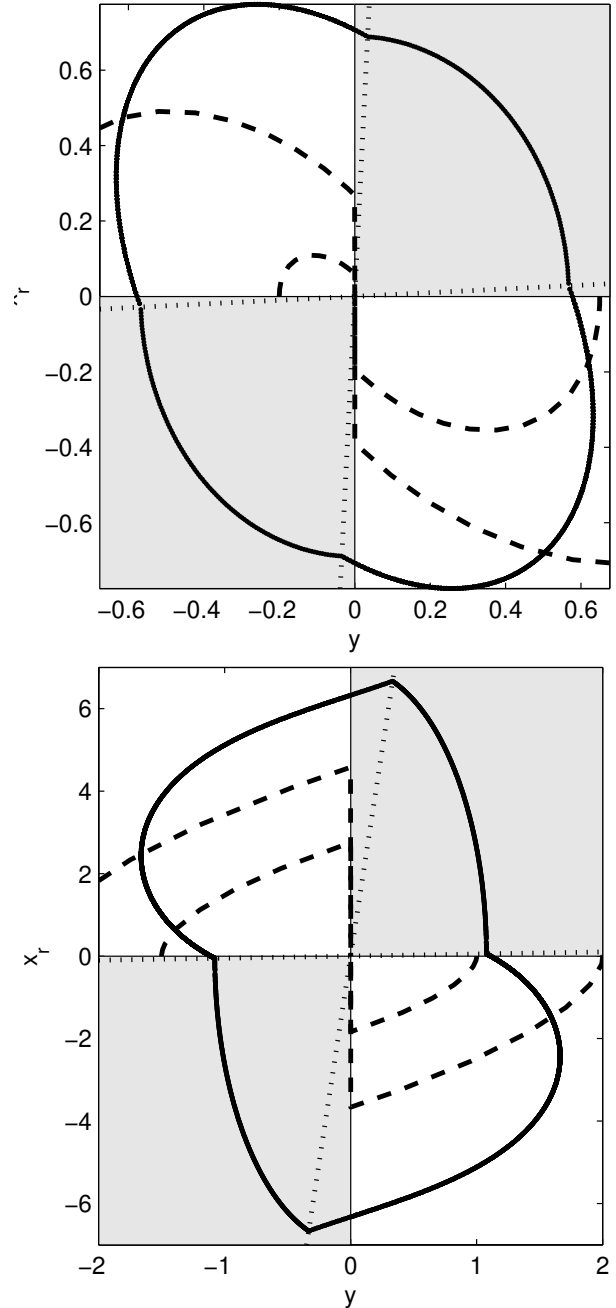


Fig. 4. Level sets of the two Lyapunov functions proposed in Theorem 1 and trajectories of the closed-loop (selecting  $\theta_\varepsilon = 0.05$ ). Top:  $\lambda_r = -1$ . Bottom:  $\lambda_r = 1$ .

*Proof of Theorem 1.* The proof consists in proposing two Lyapunov functions (one for each one of the two bounds

in (7)) which satisfy the conditions in Theorem 1 and, as  $\rho \rightarrow 0$ , provide the two bounds. In particular, as illustrated in the level sets reported in Figure 4, both functions are defined as follows:

$$V(x) := \begin{cases} V_f(x), & \text{if } x^T M_{\theta_\varepsilon} x \geq 0, \\ x^T \hat{P} x, & \text{if } x^T M_{\theta_\varepsilon} x \leq 0, \end{cases} \quad (9)$$

where  $x := (y, x_r)$ ,  $\theta_\varepsilon$  is a small enough angle and  $M_{\theta_\varepsilon} := \begin{bmatrix} \sin(2\theta_\varepsilon) & -1 \\ -1 & \sin(2\theta_\varepsilon) \end{bmatrix}$  is associated with the white regions in Figure 4, corresponding to the second and fourth quadrant inflated by an angle  $\theta_\varepsilon$ . Given the selection (9), we will next propose two smooth selections of  $V_f(\cdot)$  which are both positive definite in  $\{x : x^T M_{\theta_\varepsilon} x \geq 0\}$  and that provide, respectively, the two bounds in (7).

The matrix  $\hat{P}$  is selected so that continuity of  $V(\cdot)$  is ensured and the jump condition at item 4 is satisfied (this is always possible for any smooth  $V_f(\cdot)$  which is positive definite in  $\{x : x^T M_{\theta_\varepsilon} x \geq 0\}$  and for a small enough  $\theta_\varepsilon$ ). In particular, we pick  $\hat{P}$  diagonal with the following diagonal entries:

$$\begin{bmatrix} \hat{p}_1 \\ \hat{p}_2 \end{bmatrix} = \begin{bmatrix} \cos^2 \theta_\varepsilon & \sin^2 \theta_\varepsilon \\ \sin^2 \theta_\varepsilon & \cos^2 \theta_\varepsilon \end{bmatrix}^{-1} \begin{bmatrix} v_1 \\ v_2 \end{bmatrix} \quad (10)$$

where  $v_1 := V_f^2((\cos \theta_\varepsilon, \sin \theta_\varepsilon))$  and  $v_2 := V_f^2((\sin \theta_\varepsilon, \cos \theta_\varepsilon))$  are the values of  $V_f(\cdot)$  on the patching hyperplanes.

*Bound for  $\lambda_r < 0$ .* We first prove the first bound in (7). Consider the quadratic function

$$V_f(x) := x^T P x := x^T \begin{bmatrix} -\frac{2+\lambda_r^2}{\lambda_r} & 1 \\ 1 & -\frac{2}{\lambda_r} \end{bmatrix} x, \quad (11)$$

which is positive definite for any  $\lambda_r < 0$ . The arising function  $V(\cdot)$  according to (9) is Lipschitz by smoothness and by the continuity enforced in (10).<sup>1</sup> Moreover, it trivially satisfies items 1 and 2 of Theorem 1. To show the remaining item 3 of Theorem 1, compute the derivative of  $V_f(\cdot)$  along the dynamics of (6), (2), (3) (with  $k = 1$ ) and complete squares as follows:

$$\begin{aligned} \dot{V}_f &= -|y|^2 - |x_r|^2 - \frac{2+\lambda_r^2}{\lambda_r} y d + x_r d \\ &\leq -|y|^2 - |x_r|^2 + \gamma \left( \frac{y^2}{2\gamma} + \frac{\gamma d^2}{2} \right) + \left( \frac{2x_r^2}{2} + \frac{d^2}{4} \right) \\ &\leq -\frac{|y|^2}{2} + \frac{\gamma^2}{2} |d|^2, \end{aligned}$$

where  $\gamma := \frac{2+\lambda_r^2}{\lambda_r}$ . Then the first bound in (7) follows from Theorem 1 by picking  $\varepsilon_S$  in item 3 arbitrarily small and using the scaled Lyapunov function  $\tilde{V} := \frac{2}{\gamma} V$ .

*Bound for  $\lambda_r > -\frac{4}{\pi}$ .* For positive values of  $\lambda_r$ , the underlying linear dynamics of the reset system are exponentially unstable. Therefore, the technique used in the previous bound will not work, as there's no quadratic function which

decreases along the closed-loop trajectories. Instead, we will use a function which becomes increasingly large in the second and fourth quadrants and continuity will be ensured by the quadratic function given by  $\hat{P}$  in the first and third quadrants. To define  $V_f(\cdot)$ , it will be convenient to write the dynamics in polar coordinates  $(r, \theta)$ , with the following implicit definitions:

$$\begin{aligned} y &= r \cos \theta, \\ x_r &= r \sin \theta. \end{aligned} \quad (12)$$

Then, the flow dynamics of the closed-loop can be written as follows (see also [14, §10.5]):

$$\begin{aligned} \dot{r} &= d \cos \theta + \lambda_r r \sin^2 \theta \\ \dot{\theta} &= -1 - r^{-1} d \sin \theta + \lambda_r \sin \theta \cos \theta. \end{aligned} \quad (13)$$

Consider now the following selection:

$$V_f := \begin{cases} \frac{1}{2} r^2 \varphi(\theta), & \text{if } \theta \in [\frac{\pi}{2} - \theta_\varepsilon, \pi + \theta_\varepsilon], \\ \frac{1}{2} r^2 \varphi(\theta - \pi), & \text{if } \theta \in [\frac{3\pi}{2} - \theta_\varepsilon, 2\pi + \theta_\varepsilon]. \end{cases} \quad (14)$$

where  $\varphi(\cdot)$ , to be selected later, is such that there exist scalars  $\varphi_M > \varphi_m > 0$  satisfying  $\varphi_m \leq \varphi(\theta) \leq \varphi_M$  for all  $\theta \in \mathcal{T} := [\frac{\pi}{2} - \theta_\varepsilon, \pi + \theta_\varepsilon]$ . Then the arising  $V(\cdot)$  according to (9) trivially satisfies items 1 and 2 of Theorem 1. Moreover, by the symmetry in (14) and by the linearity of the flow dynamics, we only need to show item 3 for the inflated second quadrant, namely for  $\theta \in \mathcal{T}$ .

Here we propose the following selection of  $\varphi(\cdot)$

$$\varphi(\theta) = \varphi_0(\theta) + \varphi_\varepsilon(\theta), \quad (15a)$$

where for any small  $\varepsilon > 0$ , picking

$$\varphi_0(\theta) := \theta - \frac{\pi}{2} + \frac{1}{2} \sin 2\theta \quad (15b)$$

$$\varphi_\varepsilon(\theta) := \varepsilon \left( \frac{1}{2 \max\{|\lambda_r|, 1\}} - \sin \theta \cos \theta \right) \quad (15c)$$

ensures that<sup>2</sup> there exists a small enough  $\theta_\varepsilon$  such that the uniform lower and upper bounds on  $\varphi(\cdot)$  exist.

Consider now the derivative of the Lyapunov function (14), (15) along the dynamics (13). We will first consider the simplified case with  $\varepsilon = 0$ , so that  $V_f(\theta) = V_{f0}(\theta) := \frac{1}{2} r^2 \varphi_0(\theta)$  for all  $\theta \in \mathcal{T}$ , and then comment on how to extend the result to the general setting. After some simplifications, we get

$$\begin{aligned} \dot{V}_{f0} &= -r^2 \cos^2 \theta + dr \cos \theta \left( \theta - \frac{\pi}{2} \right) \\ &\quad + \frac{\lambda_r}{2} r^2 \sin \theta \left( (2\theta - \pi) \sin \theta + 2 \cos \theta \right), \end{aligned} \quad (16)$$

First consider  $\lambda_r \geq 0$ , which leads to the left term in the maximum at the second line of (7). Note that

$$g(\theta) := (2\theta - \pi) \sin \theta + 2 \cos \theta \leq 0, \quad \forall \theta \in \left[ \frac{\pi}{2}, \pi \right], \quad (17)$$

because  $g(\frac{\pi}{2}) = 0$  and  $\frac{dg(\theta)}{d\theta} = (2\theta - \pi) \cos \theta \leq 0$ , for all  $\theta \in [\frac{\pi}{2}, \pi]$ . Then, since also  $\sin \theta \geq 0$  for all  $\theta \in [\frac{\pi}{2}, \pi]$ ,

<sup>1</sup>A level set of this Lyapunov function for  $\lambda_r = -1$  and  $\theta_\varepsilon = 0.1$  is shown in the left plot of Figure 4.

<sup>2</sup>A level set of this Lyapunov function for  $\lambda_r = 1$ ,  $\theta_\varepsilon = 0.05$  and  $\varepsilon = 0.1$  is shown in the right plot of Figure 4.

the last term at the right hand side of (16) is negative and, using (12) we get

$$\dot{V}_{f0} \leq -|y|^2 + |x_1||d| \max_{\theta \in [\frac{\pi}{2}, \pi]} \left( \theta - \frac{\pi}{2} \right) \quad (18)$$

$$= -|y|^2 + \frac{\pi}{2}|x_1||d|, \quad (19)$$

which implies the result by completion of squares and suitable scaling  $V_{f0}(\cdot)$ .

Consider now the case  $-\frac{4}{\pi} < \lambda_r < 0$ . By borrowing some negativity from the first term at the right hand side, equation (16) can be rewritten as

$$\dot{V}_{f0} = -\left(\frac{4+\lambda_r\pi}{4}\right)r^2\cos^2\theta + dr\cos\theta\left(\theta - \frac{\pi}{2}\right) + r^2\bar{g}(\theta), \quad (20)$$

where  $\bar{g}(\theta) := \frac{\lambda_r\pi}{4}\cos^2\theta + \frac{\lambda_r}{2}\sin(\theta)g(\theta)$ . Then we have  $\bar{g}(\frac{\pi}{2}) = 0$  and,

$$2\frac{d\bar{g}(\theta)}{d\theta} = 2\lambda_r(\theta - \pi)\cos\theta\sin\theta + \lambda_r g(\theta)\cos\theta \leq 0, \quad \forall \theta \in \left[\frac{\pi}{2}, \pi\right], \quad (21)$$

because  $\lambda_r \leq 0$  and, also by (17),  $\cos\theta \leq 0$  and  $g(\theta) \leq 0$  in  $[\frac{\pi}{2}, \pi]$ . Then the last term on the right hand side of (20) is negative and, similar to the derivation in (19), using the polar coordinates transformation (12), the following bound holds:

$$\frac{4}{4 + \lambda_r\pi}\dot{V}_{f0} \leq -|y|^2 + \frac{2\pi}{4 + \pi\lambda_r}|x_1||d|, \quad (22)$$

which implies the bound at the right hand side of the second equation of (7) by scaling  $V_{f0}$  and by completion of squares.

We consider now the case with  $\theta_\varepsilon > 0$  and use the function  $\varphi_\varepsilon(\theta)$  introduced in (15c) to guarantee positive definiteness of  $V_f(\cdot)$  and to guarantee the decrease condition at item 3 of Theorem 1 for small enough  $\varepsilon_S > 0$  and  $\varepsilon_M > 0$  (namely,  $\theta_\varepsilon$ ). To this aim, consider the derivative  $\dot{V}_{f\varepsilon}$  of the function  $V_{f\varepsilon}(r, \theta) := \frac{1}{2}r^2\varphi_\varepsilon(\theta)$  along the system dynamics for  $\theta \in \mathcal{T}$  and note that since  $\dot{V}_f = \dot{V}_{f0} + \dot{V}_{f\varepsilon}$ , it is sufficient that  $\dot{V}_{f\varepsilon}$  provides an extra negative term of the type  $-\varepsilon\eta r^2 \sin^2\theta$  in the  $\dot{V}_f$  equation. As a matter of fact, half of that term will be used to provide the  $-\varepsilon_S|x|^2$  (when combined with a small amount of the  $-r^2\cos^2\theta$  term of (16)). Moreover, the remaining half will be used to complete squares with mixed terms of the form  $\sin\theta\cos\theta$  arising both from  $\theta_\varepsilon$  and  $\varphi_\varepsilon(\theta)$  (part of the  $-r^2\cos^2\theta$  will also be used in the completion of squares). To avoid overwhelming the notation of the proof with unnecessary technicalities, we only mention here that after some calculations and suitable simplifications,  $\dot{V}_{f\varepsilon}$  satisfies for all  $\theta \in \mathcal{T}$

$$\dot{V}_{f\varepsilon} \leq \frac{\varepsilon}{2} \left( -\frac{1}{2}r^2\sin^2\theta + rd \left( \frac{1}{2\max\{|\lambda_r|, 1\}} \cos\theta - \sin\theta \right) - \lambda_r r^2 \cos\theta \sin\theta + r^2 \cos^2\theta \right),$$

which is sufficient to complete the proof. •

## V. CONCLUSIONS

In this paper we analyzed stability and performance of a First Order Reset Element (FORE) connected to an integrator. We first proved exponential stability of the closed-loop system and then provided an estimate of the  $\mathcal{L}_2$  gain from a disturbance acting at the plant input to the plant output. Interesting conclusions could be drawn about the performance trend for asymptotic behavior of the pole of the FORE.

## REFERENCES

- [1] O. Beker, C.V. Hollot, and Y. Chait. Plant with an integrator: an example of reset control overcoming limitations of linear feedback. *IEEE Transactions on Automatic Control*, 46:1797–1799, 2001.
- [2] O. Beker, C.V. Hollot, and Y. Chait. Fundamental properties of reset control systems. *Automatica*, 40:905–915, 2004.
- [3] Y. Chait and C.V. Hollot. On Horowitz's contributions to reset control. *Int. J. Nonlin. Rob. Contr.*, 12:335–355, 2002.
- [4] Q. Chen, Y. Chait, and C.V. Hollot. Analysis of reset control systems consisting of a FORE and second order loop. *J. Dynamic Systems, Measurement and Control*, 123:279–283, 2001.
- [5] Q. Chen, C.V. Hollot, and Y. Chait. Stability and asymptotic performance analysis of a class of reset control systems. In *IEEE Conf. Decis. Contr.*, pages 251–256, Sidney, Australia, 2000.
- [6] J.C. Clegg. A nonlinear integrator for servomechanisms. *Trans. A.I.E.E.*, 77 (Part II):41–42, 1958.
- [7] A. Feuer, G.C. Goodwin, and M. Salgado. Potential benefits of hybrid control for linear time invariant plants. In *Amer. Contr. Conf.*, pages 2790–2794, Albuquerque, New Mexico, 1997.
- [8] R. Goebel, J. Hespanha, A.R. Teel, C. Cai, and R. Sanfelice. Hybrid systems: generalized solutions and robust stability. In *NOLCOS*, 2004.
- [9] C.V. Hollot, O. Beker, Y. Chait, and Q. Chen. On establishing classic performance measures for reset control systems. In S.O. Moheimani, editor, *Perspectives in robust control*, Lect. Notes Contr. Info. Sci. 268, pages 123–147, London, 2001. Springer Verlag.
- [10] C.V. Hollot, Y. Zheng, and Y. Chait. Stability analysis for control systems with reset integrators. In *Conf. Decis. Contr.*, pages 1717–1719, San Diego, California, 1997.
- [11] I. Horowitz and P. Rosenbaum. Non-linear design for cost of feedback reduction in systems with large parameter uncertainty. *Int. J. Contr.*, 21:977–1001, 1975.
- [12] H. Hu, Y. Zheng, Y. Chait, and C.V. Hollot. On the zero inputs stability of control systems with Clegg integrators. In *Amer. Contr. Conf.*, pages 408–410, Albuquerque, New Mexico, 1997.
- [13] K.H. Johansson, J. Lygeros, S. Sastry, and M. Eggerstedt. Simulation of Zeno hybrid automata. In *Conference on Decision and Control*, pages 3538–3543, Phoenix, Arizona, 1999.
- [14] H.K. Khalil. *Nonlinear Systems*. Prentice Hall, USA, 3rd edition, 2002.
- [15] K.R. Krishnan and I.M. Horowitz. Synthesis of a non-linear feedback system with significant plant-ignorance for prescribed system tolerances. *Int. J. Contr.*, 19:689–706, 1974.
- [16] D. Nešić, L. Zaccarian, and A.R. Teel. Stability properties of reset systems. In *IFAC World Congress*, Prague, Czech Republic, July 2005.
- [17] L. Zaccarian, D. Nešić, and A.R. Teel. First order reset elements and the Clegg integrator revisited. In *Proc. of the American Control Conference*, pages 563–568, Portland (OR), USA, June 2005.